HHS Public Access

Author manuscript

Cryobiology. Author manuscript; available in PMC 2017 September 19.

Published in final edited form as:

Cryobiology. 2009 February ; 58(1): 12–19. doi:10.1016/j.cryobiol.2008.09.013.

Biophysics of Zebrafish (*Danio rerio*) Sperm

M. Hagedorn[1,2], **J. Ricker**[3], **M. McCarthy**[3], **S.A. Meyers**[3], **T.R. Tiersch**[4], **Z. M. Varga**[5], and **F.W. Kleinhans**[6]

[1]Department of Reproductive Sciences, Smithsonian National Zoological Park, Washington, D.C. 20008

[2]Hawaii Institute of Marine Biology, University of Hawaii, Kaneohe, HI 96744

[3]Department of Anatomy, Physiology & Cell Biology, University of California at Davis, Davis, CA 95616

[4]Aquaculture Research Station, Louisiana State University Agricultural Center, Louisiana Agricultural Experimental Station, Baton Rouge, LA 70803

[5]Zebrafish International Resource Center, University of Oregon, Eugene, OR 97403

[6]Department of Physics, Indiana University-Purdue University Indianapolis, Indianapolis, IN 46202

Abstract

In the past two decades, laboratories around the world have produced thousands of mutant, transgenic, and wild-type zebrafish lines for biomedical research. Although slow-freezing cryopreservation of zebrafish sperm has been available for 30 years, current protocols lack standardization and yield inconsistent post-thaw fertilization rates. Cell cryopreservation cannot be improved without basic physiological knowledge, which was lacking for zebrafish sperm. The first goal was to define basic cryobiological values for wild-type zebrafish sperm and to evaluate how modern physiological methods could aid in developing improved cryopreservation protocols. Coulter counting methods measured an osmotically inactive water fraction (Vb) of 0.37 ± 0.02 (SEM), an isosmotic cell volume (Vo) of 12.1 ± 0.2 μm^3 (SEM), a water permeability (Lp) in 10% dimethyl sulfoxide of 0.021 ± 0.001(SEM) um/min/atm, and a cryoprotectant permeability (Ps) of 0.10 +/− 0.01 (SEM) × 10^{-3} cm/min. Fourier transform infrared spectroscopy indicated that sperm membranes frozen without cryoprotectant showed damage and lipid reorganization, while those exposed to 10% glycerol demonstrated decreased lipid phase transition temperatures, which would stabilize the cells during cooling. The second goal was to determine the practicality and viability of shipping cooled zebrafish sperm overnight through the mail. Flow cytometry demonstrated that chilled fresh sperm can be maintained at 92% viability for 24 h at 0°C, suggesting that it can be shipped and exchanged between laboratories. Additional methods will be necessary to analyze and

Correspondence and requests for materials should be addressed to: Dr. M. Hagedorn, Smithsonian Institution and Hawaii Institute of Marine Biology, P. O. Box 1346, Kaneoehe, HI 96744, hagedornm@si.edu, 808-520-1346 (TEL), 808-236-7444 (FAX).

improve cryopreservation techniques and post-thaw fertility of zebrafish sperm. The present study is a first step to explore such techniques.

Keywords

Coulter; Fourier Transform Infrared Spectroscopy; permeability; cell membrane; lipid; cryopreservation; freeze damage; osmotic pressure; zebrafish; *Danio rerio*

Introduction

In the past two decades, laboratories around the world have produced thousands of mutant, transgenic, and wild-type zebrafish lines, but maintaining all of them alive is expensive, inefficient, and beyond the capacity even of stock centers. Thus, the risk exists that many of these valuable research resources become extinct if they cannot be properly preserved for future generations. The pace of science is exceeding our ability to maintain and store important genetic strains. This trend has also been observed in other important animal model systems, such as the mouse, where more than 3,000 knockout strains and over 28,000 mutant strains exist, and the costs of maintaining these large numbers are becoming overwhelming [17].

Most technological innovations in the field of germplasm cryopreservation arose from a sound understanding of the mechanisms of cryodamage and cryoprotection [18, 19]. Successful cryopreservation of germplasm must consider intrinsic biophysical properties (e.g., water and cryoprotectant permeability, osmotic tolerance limits, intracellular ice nucleation) to maximize survival [24]. A systematic approach, using fundamental cryobiological principles, is vital to improving post-thaw fertilization for fish sperm. It is important to understand and avoid the mechanisms by which sperm is damaged or destroyed during cryopreservation. However, no fundamental cryobiological data on which a systematic approach could be based is known for zebrafish sperm, and only a limited number of biophysical parameters have been studied for fish sperm [22, 28, 29, 6].

Although slow-freezing cryopreservation is a proven method for long-term maintenance of genetic material, current protocols in use by the zebrafish community are not standardized, yield inconsistent results, and threaten the efficacy of large-scale genetic screening, the integrity of individual laboratory lines, and the functioning of stock centers. Several problems have been identified with regard to zebrafish sperm cryopreservation. Most cryopreservation protocols currently used by the zebrafish research community are more than 25 years old, empirical in nature and relatively difficult to learn. Success rates and fertilization rates vary considerably among laboratories, and most protocols are modifications from a single cryopreservation procedure [11] adapted in various ways by the zebrafish community [30, 21, 7, 27]. Currently, there are approximately 7,000 wild-type, mutant and transgenic strains of zebrafish in need of adequate preservation.

At a recent workshop held at the National Institutes of Health on “Achieving High-throughput Repositories for Biomedical Germplasm Preservation”, a number of model systems were compared in terms of their status and variety of cryopreserved genetic

materials, such as sperm, embryos, oocytes, and stem cells [20]. Aquarium fish rated the lowest compared to all the other model systems, including mouse, rat, and non-human primates, because currently the only option for long-term storage of genetic material is sperm cryopreservation. Moreover, sperm cryopreservation of aquarium fish relies on variable and unreliable protocols. This meant that cryopreserved fish material was poorly represented compared to the genetic material available in other research communities, and that many research resources are in danger to be lost for future generations. Therefore, improvements and modifications of current protocols are critical to enable high-throughput cryopreservation for fish genetic material. Although it was recognized at the workshop that standard cryobiological values are important for designing cryopreservation protocols, it was pointed out that newer tools that help evaluate the physiological status of whole cells and organelles before freezing and after thawing were particularly needed.

The first goal of this study was to begin to define basic cryobiological values for wild-type zebrafish sperm, and to assess modern physiological approaches that could yield practical information to help improve cryopreservation methods. These improved methods and values, we determined in this study, could become important for wild-type, inbred, and mutant strains that are otherwise difficult to cryopreserve with current methods. We collected basic information on wild-type (WIK) sperm, including the osmotically inactive component (Vb) of the cell, the water and cryoprotectant permeability (Lp and Ps), and the viability of sperm that had been chilled and transported. In addition, we analyzed zebrafish sperm membranes with Fourier transform infrared spectroscopy (FTIR). This is an established tool for biophysical characterization of cell membranes [4] that is extremely sensitive to changes in lipid conformational order, and allows for measurement of membrane fluidity and lipid organization in intact cell membranes. We report preliminary studies on the application of FTIR to zebrafish sperm membranes, and show that it is useful for studying fundamental biophysical properties of membranes and diagnosing damage due to freezing and thawing the sperm.

The second goal was to test whether sperm could be stored on ice over extended periods and maintains vital values. This is of particular practical interest for zebrafish sperm cryopreservation because new strategies can be developed for more time-efficient collection and storage of large numbers of samples, and samples can also be shipped by mail and exchanged between laboratories for in vitro fertilization or cryopreservation.

Materials and Methods

Collection of sperm

All zebrafish were obtained from the Zebrafish International Resource Center (www.zfin.org), and the team collected the sperm through non-survival surgical excision of testes following euthanasia of males by overdose of MS-222 (tricaine). All sperm measurements were made by a team located at UC Davis on fresh sperm, except for one study where the sperm was sent from Hawaii 24 h through the mail to UC Davis for a viability assessment and a single FTIR experiment. Briefly, males were immersed in a 0.02% solution of tricaine methane sulfonate until gill movements stopped, and the animals no longer responded to gentle touch. The males were rinsed with clean aquarium water and

placed on a damp sponge in ventral recumbency and quickly decapitated to prevent further pain or stress. The anal area was dried, and an incision made to open the peritoneal cavity. The testes were removed from both sides, crushed with forceps to release the sperm, and placed into chilled Hanks' balanced salt solution (HBSS) at 300 mOsm/kg (0.137 M NaCl, 5.4 mM KCl. 1.3 mM $CaCl_2$, 1.0 mM $MgSO_4$, 0.25 mM Na_2HPO_4, 4.2 mM $NaHCO_3$ and 5.55 mM glucose, pH 7.2) to maintain the sperm and prevent activation. Sperm solutions were maintained on ice prior to all experiments. Wild-type WIK-strain spermatozoa from 3 to 4 males were pooled in each experiment. All care and welfare for the animals met NIH animal care standards.

Morphology

Zebrafish sperm were activated at 200 mOsm/kg and their concentration and swimming patterns determined using computer-assisted semen analysis software (IVOS, Hamilton Thorne Bioscience, Beverly, MA). Cells were imaged on an Olympus BX-60 fluorescent microscope with a Zeiss Axiocam® camera with AxioVision® software (Carl Zeiss Vision, GmbH, Aalen, Germany). For permeability measurements, the volume-to-area ratio is necessary, and the scanning electron microscopic sperm morphology data of Wolenksi and Hart [32] were used as the basis for this analysis. In addition, fresh sperm was used to corroborate these published data. Digital images of 10 sperm from 5 different males were captured with an Olympus BX41 microscope with an attached digital camera (Sony DFWV300) and measured with NIH Image software (version1.65, freeware). With these data, we calculated the area; however, because the Coulter and microscopic methods are subject to different errors we had to compensate for these errors by using a volume to area (V/A) ratio from the microscopic measurements. To this end, we assumed that the sperm head and midpiece are prolate spheroids, and the tail is a cylinder. The V/A ratio was applied to the Coulter volume to determine the corresponding sperm area. Thus, we associated an area with the Coulter measurements, A_c, given by the Coulter volume, V_c, divided by the microscopic volume to area ratio $(V/A)_m$. Using the (V/A) ratio had the advantage of minimizing systematic errors that may affect the microscopic and Coulter counter measurements.

Physiological Measurements

Two important cryobiological characteristics of the cell are the water (Lp) and cryoprotectant permeability (Ps). To measure them, one needs to determine the rate of change in cell volume when the cells are placed in cryoprotectant solutions. This was a dynamic measurement of volume versus time. In addition, our analysis model assumed that the cells behaved as ideal osmometers. To test this, we measured the static cell volume after the cells osmotically equilibrated with external test medium. Both of these measurements were made using a Coulter counter. We used a Beckman-Coulter Multisizer 3 particle counter in conjunction with biophysical modeling. This instrument, with beta software, allowed accurate static and dynamic (volume versus time) sperm measurements. A 50-μm aperture tube was used and calibrated with 16 μm beads in Isoton II (sample fluid from manufacturer) according to the Coulter manual. Calibration test runs done in solutions of different ionic and cryoprotectant strength indicated that this calibration held to +/− 5% in volume for the solutions used here.

To determine the non-osmotic portion of the zebrafish sperm volume (Vb), we used the Boyle van't Hoff (BVH) analysis in which volume is plotted versus the reciprocal osmolality of the test solutions (HBSS prepared at ~200, 300, and 600 mOsm/kg). In these plots, the y-axis intercept is Vb. Briefly, 2 to 8 μl of concentrated sperm (100 to 500 million cells/ml in HBSS 300 mOsm/kg) were mixed into 10 ml of the test medium and measured in the Coulter counter at 2 min after exposure. Initially, we repeated measurements over 15 min and found that a 2-min exposure was sufficient for equilibration; no volume changes occurred after this time under these conditions.

Cells that are loaded to equilibrium with a permeating cryoprotectant and then abruptly returned into buffer lacking the cryoprotectant, will increase in volume as the external water flows back into the cell, yielding a measure of Lp, followed by a slower outflow of cryoprotectant from the cell as it returns to normal volume, yielding a measure of Ps. Therefore, to determine the water and solute permeability of sperm cells in cryoprotectants, we exposed them to 10% solutions (V/V) of cryoprotectants (methanol, N,N-dimethylformamide, or dimethyl sulfoxide in 300 mOsm/kg HBSS buffer) chosen from those commonly in use in zebrafish cryopreservation or cryopreservation of other cells. After loading the sperm for 20 min with the cryoprotectant, the cells were returned to the isotonic buffer and the dynamic volume versus time changes were recorded as cryoprotectant diffused out of the cells.

Briefly, 90 ml of HBSS 300 mOsm/kg buffer were placed into a Coulter-mixing chamber that rapidly mixed added solutes. Approximately 10 μl of a concentrated sperm sample (~50 × 10^8 cells/ml), equilibrated with a test cryoprotectant, were added about 3 to 5 sec after the Coulter counter began sampling. A 20 min time frame was chosen for the study, because this is often the time needed to handle sperm during cryopreservation protocols prior to freezing. After a brief mixing artifact (~1 sec), sperm volume versus time data were acquired, and sampling continued for 120 sec.

The Coulter volume-versus-time data were analyzed as described in Hagedorn et al. [10]. Specifically a two-parameter permeability model was used with the form:

$$\mathrm{dVw/dt} = \mathrm{Lp} * \mathrm{A} * \mathrm{R} * \mathrm{T} * \Delta(\mathrm{Osm})$$

and

$$\mathrm{dns/dt} = \mathrm{Ps} * \mathrm{A} * \Delta(\mathrm{molality\ of\ cryoprotectant})$$

where V_w is the intracellular water volume and n_s is the osmoles of cryoprotectant; Lp and Ps are the previously introduced permeability coefficients, A is the cell area, R the gas constant, T the absolute temperature, and Δ(Osm) and Δ(molality of cryoprotectant) are the gradient driving forces across the cell membrane for water and cryoprotectant.

Because the beta software for the dynamic data collection on the Coulter counter did not have the appropriate noise reduction (see Results for details), large noise spikes, for examples from debris or clumped cells, were removed from the raw data manually in Microsoft Excel, and the data averaged to yield a maximum of 20 to 30 volume measurements over 120 sec. To determine the membrane permeability, the permeability

equations were numerically integrated using the Episode method for stiff differential equations and least-squares fit to the data as implemented in the software program Scientist (Micromath, St Louis, MO). The sperm area was fixed at its value in isotonic solutions. In the static Boyle van't Hoff experiments, cell volume was determined by analyzing the histogram of cell counts versus the size distribution. These histograms were transferred into Microsoft Excel; a cubic polynomial was fit to the frequency-size distribution of the sample and the peak of the polynomial was selected as the cell volume. These methods are similar to those used by Gilmore et al. [9] to analyze human sperm.

Cell Viability

Using the methods of Segovia et al. [26, 3], we measured sperm viability with live/dead fluorescent stains, specifically propidium iodide and SYBR-14 (Live/Dead Sperm Viability Kit, L-7011, Invitrogen), and flow cytometry for cells that had been held stationary in the laboratory at 0°C for 24 h or had been shipped by overnight express at 0°C for 24 h. Generally, for laboratory tests, sperm from the testes from 3 to 4 males were pooled and suspended in 20 μl of HBSS at 300 mOsm/kg/testes were used. Only one shipment of testes was performed. The testes from 4 males were excised, suspended in 80 μl of HBSS at 300 mOsm/kg, and sent chilled (0°C) via express mail. Because a flow cytometer was not available at the site of origin, no pre-shipment measurements were possible.

To determine the flow cytometric properties of the population of zebrafish sperm to be analyzed, a sample of 100% damaged cell membranes was generated by boiling an aliquot of sperm for 10 min. This sample was stained with propidium iodide (PI) only. With all sperm stained red, as confirmed by fluorescence microscopy, the entire population of zebrafish sperm could be identified and gated (or restricted to certain channels) accordingly for the remaining experiments.

For determination of sperm viability (i.e., membrane integrity) cells were diluted to 25×10^6/mL in 300 mOsm HBSS and incubated at RT for 5 min with SYBR-14 (0.l μM final concentration) followed by an additional 5 min incubation with PI (final concentration 12 μM) (Live/Dead Sperm Viability Kit, L-7011, Invitrogen). SYBR-14 may fuse with exogenous lipids labeling live sperm with green fluorescence, and PI is a membrane-impermeant nucleic acid stain that labels membrane-compromised sperm with red fluorescence. The PI interchalates with DNA which gives the red fluorescence, but this happens only if the cell membranes are broken and it can diffuse into the cell nucleus. After incubation, samples were diluted to 1×10^6cells/mL and immediately assessed by flow cytometry (FACScan; Becton-Dickinson, Franklin Lakes, NJ, USA with a Macintosh interface). A total of 10,000 gated events were analyzed for each sample with a running rate of approximately 300–500 events/sec. A 488-nm filter was used for excitation of both SYBR-14 and PI with a 535-nm and a 595-nm emission filter used to quantify green and red fluorescence respectively. Frequency plots were prepared to determine the percent of the population that stained positively with SYBR-14 and PI. The population of cells in the lower right quadrant exhibited intact membranes, while those in the upper right and left quadrants the populations were damaged.

Behavior of Membrane Lipids

Using the FTIR methods of Ricker et al. [25], some biophysical characteristics of zebrafish sperm membranes in fresh, thawed, and cryoprotectant-treated samples were examined. Approximately 15 μl of highly concentrated sperm (50×10^8cells/ml or higher) either diluted with HBSS (300 mOsm/kg) or a 10% (V/V) solution of cryoprotectant (i.e., glycerol, DMSO or N,N-dimethyl formamide) in HBSS 300 mOsm/kg) were spread onto CaF_2 windows for analysis. Data were obtained with a Spectrum 2000 Fourier Transform Infrared spectrometer with Spectrum 3.1 software (Perkin Elmer, Norwalk, CT). The instrument was purged of water vapor with dry air and the sample temperature controlled by a Peltier device and monitored with a thermocouple. Temperature was ramped at 2°C/min for all samples, and a total of 16 spectra were averaged for each data point. The lipid CH_2 stretching region was analyzed. Phase transitions were determined by plotting lipid CH_2 bands as a function of temperature and taking the first derivative (smoothed) of the data. Figures 6 represent typical plots.

Results

Morphology and Swimming Behavior

Zebrafish sperm have small, round heads and a smaller mid-piece (Fig. 1) that together were approximated as a prolate spheroid. Using light microscopy on fresh material, the average major and minor axes of the combined head and mid-piece were 2.2 μm ± < 0.1 μm (SEM) and 1.9 μm ± < 0. 1m, an average tail length of 27.6 μm ± 0.5 μm with an average tail thickness of 0.4 μm ± < 0.1 μm in diameter. The scanning micrographs of Wolenski and Hart [32] showed the sperm head and mid-piece in greater detail with a major axis of 2.4 μm and a minor axis of 1.8 μm, with delicate tails, 30 μm long × 0.4 μm in diameter. These latter dimensions were used to yield a microscopically determined volume of 7.8 μm^3, an area of 53 μm^2, and a volume to area ratio (V/A) = 0.148 μm.

Physiological Measurements

In the two-parameter permeability model, the osmotically inactive cell volume (Vb) is required to convert the Coulter cell volume measurements to the cell water volume. Additionally, to compute cell ionic and cryoprotectant concentrations in the model, we assumed that the cells behaved as ideal osmometers i.e., they obeyed a Boyle van't Hoff relationship. To determine Vb of zebrafish sperm, four experiments were done over 3 days, yielding a value of 0.37 ± 0.02 SEM and an isosmotic Coulter determined cell volume (Vo) of 12.1 ± 0.2 μm^3 (volume parameters discussed further in Discussion). This indicated that approximately 37% of the sperm cell was solids and osmotically inactive water. The osmometric behavior of the sperm was linear from approximately 200 to 600 mOsm/kg in the Boyle van't Hoff plot (Fig. 2), suggesting that these cells behave as an ideal osmometer in this osmotic range. The sperm cells displayed different volume versus time behaviors depending on the cryoprotectant tested. For example, sperm cells exposed to 10% dimethyl sulfoxide displayed a volume increase (due to water influx) followed by a volume decrease (due to water and cryoprotectant efflux) (Fig. 3). In total, water and dimethyl sulfoxide permeability were measured four times (thousands of cells/sample), yielding a value for Lp of 0.021± 0.001 μm/min/atm and one for Ps of $0.10 \times 10^{-3} \pm 0.01 \times 10^{-3}$ cm/min. In

contrast, cells exposed to 10% methanol and 10% N,N-dimethyl formamide solutions showed no apparent change in volume in repeated trials as the cryoprotectant left the cells (Fig. 4). As elaborated on further in the Discussion, we believed this flat response was the result of high membrane cryoprotectant permeability. The minimum cryoprotectant permeability necessary to yield a flat line was estimated as follows. First, a value of Lp was needed for the modeling and we used the value found in the dimethyl sulfoxide experiments. We believed this was a good estimate because the water permeability is not typically found to be strongly dependent on the specific cryoprotectant present [9]. Then simulations were conducted to determine a lower limit for cryoprotectant permeability that would yield a flat line and the resulting permeability values were $Ps \geq 0.3 \times 10^{-3}$ cm/min for methanol, and $Ps \geq 0.13 \times 10^{-3}$ cm/min for N,N-dimethyl formamide.

The Coulter Counter technology has been optimized over the years for static volume measurements. However, the capability to measure volume versus time was new, still in beta testing, and lacked a filter for the oversized pulses that resulted from large debris and clumped cells. It did have a filter for the undersized pulses that resulted from small debris and cell fragments. Thus, the average volume-versus-time data were biased toward high values by the inclusion of high-volume pulses and probably explains why our dynamic data yielded a slightly higher isotonic volume than those measured in the static experiments. For example, in Fig. 4, the isotonic volume values are about 2 to 3 μm^3 higher than those reported in Table 1.

Given this probable error in the dynamic volume measurements, we evaluated what effect this error might have on Lp and Ps determinations, where dimethyl sulfoxide was the cryoprotectant. The volume error was simulated in our modeling software, and in the worst case scenario, we found that our calulated Lp could be as much as 14% too low and Ps may be as much as 3% too high. This was a relatively small error considering the typical scatter in permeability measurements of cell membranes.

Cell Viability

Generally, when using 20 μl of HBSS (300 mOsm/kg) for a single crushed testis, sperm maintained in the laboratory on ice were > 90% viable for as long as 24 h, defined as being membrane intact (measured with flow cytometry) with motility able to be activated (recorded with computer-assisted semen analysis software). We also tested whether zebrafish sperm remained sufficiently viable for use in physiological experiments after 24 h in the mail on ice. After shipping, a concentration of 58×10^8 cells/ml yielded a viability of 92%, as determined by flow cytometry, and a progressive motility of 40%, as determined by the computer-assisted semen analysis software (Fig. 5).

Behavior of Membrane Lipids

We analyzed lipid phase transitions during cooling in the absence and presence of cryoprotectants. FTIR spectroscopy showed distinct thermal events during cooling and rewarming scans of fresh (Fig. 6A) and frozen sperm (no cryoprotectant, Fig. 6B). A change in slope of the raw data (circles) over a defined temperature range indicated that a lipid phase transition had occurred. Subtle changes in the slope were difficult to distinguish by

eye, and therefore a first derivative was calculated and plotted along with the raw data. As shown by the first derivative (solid line), four lipid phase transition peaks were observed for fresh sperm in the following temperature ranges: (1) −20 to −15°C, (2) −5 to 0ºC, (3) 5 to 10°C, and (4) 25 to 30ºC (Fig. 6A). These phase transitions were consistent among all fresh samples (N = 5; 2 to 4 males combined per sample). Membranes that were frozen and thawed without cryoprotectant displayed different profiles from fresh sperm (Fig. 6B). The post-thaw membranes had characteristic indicators of freezing damage, including an upward shift in lipid phase transition temperatures, and multiple sharp peaks relative to the fresh sperm profile. Such features have been observed in sperm of other species following freezing damage [25].

When we performed a cooling scan on zebrafish sperm suspended in 10% glycerol (N = 4 samples; 2 to 4 males/sample), the lipid phase transitions occurred at lower temperatures than those of untreated sperm (Fig. 6C). This solution did not freeze at −20°C due to supercooling of the glycerol solution. These data suggest that the membranes of the cryoprotected zebrafish sperm were more fluid than those of untreated sperm.

We could not firmly assign peaks to specific lipid populations unless other methods were used to label or otherwise distinguish them (for example, using deuterated lipids). Therefore, it was not possible to correlate peaks in one sample to peaks in another sample that was treated differently. For example, a peak at −19°C in a fresh sample (Fig. 6A) does not necessarily match with a peak at −19°C in a frozen and thawed sample (Fig. 6B). We concluded that the lipids in the glycerol-treated sample had shifted down in temperature because, as a group, the peaks appeared at lower temperatures than in the untreated sample. In the glycerol-treated sperm, the highest temperature peak occurred at about 10°C, which was 10 degrees below the highest temperature peak in the untreated sample.

We also attempted to examine how methanol and N,N-dimethyl formamide interacted with zebrafish sperm membranes. Unfortunately, the FTIR signal from the methyl groups in these latter two cryoprotectants interfered with the CH_2-stretching spectral region, so data could not be obtained from these common cryoprotectants of zebrafish sperm. Dimethyl sulfoxide would have presented the same problem due to the presence of methyl groups, so we did not test this compound. In the future, analysis of methylated, cryoprotectant-treated samples may be possible by washing the samples to examine pre- freeze and post-thaw freezing damage. Nevertheless, this technique is a suitable tool to study fundamental biophysical properties of the sperm membrane, to diagnose damage as a result of freezing and thawing, and to aid in the choice of cryoprotectant and cryopreservation protocol.

Discussion

The first goal of this paper was to define some of the basic cryobiological parameters for wild-type zebrafish sperm and to evaluate how some newer physiological methods, such as those described in this manuscript, might aid in developing improved cryopreservation protocols. Because little was known about these parameters for zebrafish sperm, we began by analyzing wild-type sperm, using a number of biophysical methods. No one method can determine how to optimize the cryopreservation protocol for a cell or tissue, but a

combination of tests may help point to better techniques to improve post-thaw fertility. These data and methods become particularly important if there are mutant or transgenic strains that are difficult to cryopreserve, because comparisons among groups can help guide the adjustment of cryopreservation protocols.

Maintaining zebrafish sperm on ice offers practical possibilities for shipping and sample collection

One of the practical findings of this study was that zebrafish sperm can be sent through the mail chilled and remain viable for at least as long as 24h. Shipping sperm instead of live males is preferable for a number of reasons, live animals: 1) become stressed during shipping and this can affect the quality of the cryopreserved sperm; 2) are more costly and precarious to ship; and, 3) have the potential to threaten the biosecurity of resource centers by the transmission of diseases to other live animals. Thus, shipping of chilled sperm is a viable alternative for laboratories interested in working on the same strains, and is an especially important option for transfer of genetic material to specialized facilities with cryopreservation capabilities. In addition, chilling sperm is practical to develop novel sperm collection and freezing protocols. Currently, a sperm sample is frozen immediately after it has been collected from the male. By collecting and chilling on ice, one experimenters can focus on collection for prolonged periods, then freeze all samples at once using a controlled rate freezer. This would allow streamlining workflow and a more efficient freezing protocol in high-throughput situations, for example collection of large sample numbers at a stock center.

The cryobiological properties of zebrafish sperm will help develop novel cryopreservation protocols

The cryobiological values for zebrafish sperm were previously unknown. Zebrafish sperm have a low Vb compared to that of sperm from most mammals (Table 2). It is not known whether other fish sperm will have Vb values as low as those for zebrafish, but accurate measurements are important for cryopreservation because they determine how much osmotically active water is in the cell. Previous studies have modeled sperm of four different fish species, but had to assume values for Vb, because they were unknown [6, 28, 29, 22].

Water permeability (Lp) for zebrafish sperm is approximately low, 30-fold lower than in mammalian sperm, as might be predicted for a cell that must function in a hypotonic environment (e.g., fresh water) when fertilizing an egg. Cryoprotectant permeabilities were in the range expected for most sperm (~10^{-4} cm/min), and the volume-change curve for dimethyl sulfoxide (Fig. 3) indicated that these cells were permeated by the dimethyl sulfoxide within a few minutes. However, some cryoprotectants (10% methanol and 10%N,N-dimethylformamide) did not cause any changes in cell volume as they entered and exited the cell. At least 140,000 cells over a period of 120 sec were tested in each of these solutions, so the signal from the cells was well above the noise. Two possibilities may explain the lack of volume change with time in formamide and methanol: (1) The solute moves out almost as rapidly as water moves in, or (2) the sperm are highly impermeable to the solute. Possibility (2) is ruled out because the volume held steady for the cells, rather than shrinking in the presences of an impermeable solute. Both of these cryoprotectants have

been used successfully to cryopreserve zebrafish sperm, therefore their effectiveness is evidence that the cryoprotectants are entering the cells. A similar methanol permeability pattern (basically flat) was observed in mouse embryos and it was hypothesized that the water exiting the cells balanced the methanol entering, so no effective volume change was observed [23]. We hypothesize that the same mechanism may be occurring with zebrafish sperm. This lack of osmotically induced volume excursion may make these cryoprotectants ideal candidates for further testing with slow-freezing cryopreservation.

The microscopic data from Wolenski and Hart [32] (fixed samples) and our measurements (fresh samples) yielded a sperm volume of 7.8 μm^3 in contrast to the volume from Coulter electronic particle counter of 12.1 μm^3. Some of the microscopical error could result from the osmolality of the fixative, causing changes in the cells prior to the cross-linking of the proteins. This difference was not surprising given the small and 'difficult' shape of sperm to model. These methodologies are very different and each subject to a variety of potential systematic errors. Kleinhans et al, [16] compared the available volume measurements for human sperm using a variety of techniques, including microscopic and electronic particle counter. At that time, the reported volume of human sperm ranged from 15.4 μm^3 to 37.5 μm^3 with the smallest value being given by the microscopic measurements. In order to maintain internal consistency in each of these methodologies (Coulter and microscopic), we applied the microscopic (V/A) ratio to the Coulter volume to determine an associated Coulter area, i.e.,

$$A_c = V_c/(V/A)_m = 81.8\,\mu m^2.$$

Finally, we note that it was the product of (Area)*(Permeability) which was used in the permeability equations. Thus, accurate modeling results can be obtained, even if the Area estimate turns out to be in error.

The FTIR data suggest that freezing zebrafish sperm without cryoprotectant caused membrane damage and large-scale lipid reorganization. This is reflected in the data as an upward shift in lipid phase transition temperatures (T_m), and an increase in the number and cooperativity, or sharpness, of phase transition peaks in post-thaw samples (compare Figs. 6A and B). Changes in the peaks have been observed in sperm of other species following freezing damage [25]. Cold shock damage has been directly linked to lipid phase transitions that cause the sperm membrane to become transiently leaky, thereby compromising membrane integrity [1, 8]. In addition, cooling also causes irreversible phase separation (clustering) and rearrangement of membrane components in sperm [5,12]. During chilling, then, the key is to minimize the number and cooperativity, or sharpness, of lipid phase transitions, thus keeping the membrane fluid and structurally intact. In our studies, samples treated with glycerol showed slightly lower T_m values relative to untreated fresh sperm and smoother, or less cooperative, phase transitions (compare Figs. 6A and C). We suggest that glycerol permeates the bilayer, disrupting the order of the lipid acyl chains, thus decreasing lipid phase transition temperatures (T_ms). In this way, glycerol helps to keep the membrane more fluid during freezing, and prevents large-scale lipid rearrangement within the

membrane. Unfortunately, glycerol appears to be a relatively toxic cryoprotectant for zebrafish sperm when used over 10 min [33], and less toxic cryoprotectants, such as dimethyl sulfoxide, could not be assessed using FTIR due to signal interference. In the future, examining different spectral regions of the membrane bilayer may allow for analysis of methylated cryoprotectants. In conclusion, FTIR is a useful tool to study fundamental biophysical properties of the sperm membrane and to diagnose damage as a result of freeze-thaw.

Cryopreservation methodology has already been optimized for another, small-sized fish biomedical model [13, 14. 15, 28], the internally-fertilizing green swordtail (*Xiphophorus helleri*) by using basic biophysical information. This systematic approach resulted in a greater than 70% post-thaw motility and less than 10% variability. This achievement in a fish species, with a more complex reproductive system, points to the need and the potential success this approach will have on zebrafish genetic resources. Our data on the biophysical properties of zebrafish sperm, testing its viability when maintained on ice, and testing the feasibility of using FTIR as an additional tool for freezing damage assessment, suggests that using an ensemble of physiological tools, such as shown in our study, will help improve the success of zebrafish sperm cryopreservation.

Acknowledgments

We thank Beckman Coulter Particle Characterization Group, specifically Giovanni Presti and Andres Lobeiras, for the loan of the Multisizer 3 Coulter Counter during this project, and Dr. Sweeh Teh from the UC Davis School of Veterinary Medicine's Aquatic Toxicology Laboratory, and the two anonymous reviewers whose careful reading improved this manuscript. This work was supported by a grant from the National Institutes of Health (R01 RR016581) to SM. ZMV supported by grant P40 RR012546 from NIH-NCRR.

References

1. Agca Y, Mullen S, Liu J, Johnson-Ward J, Gould K, Chan A, Critser J. Osmotic tolerance and membrane permeability characteristics of rhesus monkey (*Macaca mulatta*) spermatozoa. Cryobiology. 2005; 51:1–14. [PubMed: 15922321]
2. Arav A, Pearl M, Zeron Y. Does lipid profile explain chilling sensitivity and membrane lipid phase transition of spermatozoa and oocytes? Cryo Letters. 2000; 21:179–186. [PubMed: 12148049]
3. Baumber J, Meyers S. Changes in membrane lipid order with capacitation in rhesus macaque (*Macaca mulatta*) Spermatozoa. Journal of Andrology. 2006; 27(4):578–87. [PubMed: 16582419]
4. Crowe JH, Hoekstra FA, Crowe LM, Anchordoguy TJ, Drobnis E. Lipid phase transitions measured in intact cells with Fourier transform infrared spectroscopy. Cryobiology. 1989; 26:76–84. [PubMed: 2924595]
5. DeLeew FE, Chen HC, Colenbrander B, Verkleij AJ. Cold-induced ultrastructural changes in bull and boar sperm plasma membranes. Cryobiology. 1990; 27:171–183. [PubMed: 2331890]
6. Devireddy RV, Campbell WT, Buchanan JT, Tiersch TR. Freezing response of white bass (*Morone chrysops*) sperm cells. Cryobiology. 2006; 52:440–445. [PubMed: 16524569]
7. Draper BW, McCallum CM, Stout JL, Slade AJ, Moens CB. A high-throughput method for identifying N-ethyl-N-nitrosourea (ENU)-induced point mutations in zebrafish. Meth Cell Biol. 2004; 77:91–112.
8. Drobnis EZ, Crowe LM, Berger T, Anchordoguy TJ, Overstreet JW, Crowe JH. Cold shock damage is due to lipid phase transitions in cell membranes: A demonstration using sperm as a model. J Exp Zool. 1993; 265:432–437. [PubMed: 8463792]

9. Gilmore JA, McGann LE, Liu J, Gao DY, Peter AT, Kleinhans FW, Critser JK. Effect of cryoprotectant solutes on water permeability of human spermatozoa. Biol Reprod. 1995; 53:985–995. [PubMed: 8527530]
10. Hagedorn M, Kleinhans FW, Artemov D, Pilatus U. Characterization of a major permeability barrier in the zebrafish embryo. Biol Reprod. 1998; 59:1240–1250. [PubMed: 9780333]
11. Harvey B, Kelley RN, Ashwood-Smith MJ. Cryopreservation of zebrafish spermatozoa using methanol. Can J Zool. 1982; 60:1867–1870.
12. Holt WV, North RD. Partially irreversible cold-induced lipid phase transitions in mammalian sperm plasma membrane domains: freeze-fracture study. J Exp Zool. 1984; 230:473–483. [PubMed: 6747573]
13. Huang C, Dong Q, Walter RB, Tiersch TR. Sperm cryopreservation of a live-bearing fish, the platyfish *Xiphophorus helleri*. Theriogenology. 2004a; 62:179–194. [PubMed: 15159112]
14. Huang C, Dong Q, Walter RB, Tiersch TR. Sperm cryopreservation of green swordtail *Xiphophorus helleri*, a fish with internal fertilization. Cryobiology. 2004b; 48:295–308. [PubMed: 15157778]
15. Huang C, Dong Q, Walter RB, Tiersch TR. Initial studies on sperm cryopreservation of a live-bearing fish, the green swordtail *Xiphophorus helleri*. Theriogenology. 2004c; 62:179–194. [PubMed: 15159112]
16. Kleinhans FW, Travis VS, Du J, Villines PM, Colvin KE, Critser JK. Measurement of human sperm intracellular water volume by electron spin resonance. J Andrology. 1992; 13:498–506.
17. Knight J, Abbot A. Full house. Nature. 2002; 417:785–786. [PubMed: 12075313]
18. Mazur P. Cryobiology: the freezing of biological systems. Science. 1970; 168:939–949. [PubMed: 5462399]
19. Mazur P. Freezing of living cells: mechanisms and implications. Am J Physiol. 1984; 247:C125–142. [PubMed: 6383068]
20. Mazur P, Leibo SP, Seidel GE Jr. Cryopreservation of the germplasm of animals used in biological and medical research: importance, impact, status, and future directions. Biol Reprod. 2008; 78(1): 2–12. [PubMed: 17901073]
21. Morris JP, Berghmans S, Zahrieh D, Neuberg DS, Kanki JP. Zebrafish sperm cryopreservation with N,N-dimethylacetimide. Biotechniques. 2003; 35:956–958. [PubMed: 14628669]
22. Pinisetty D, Huang C, Dong Q, Tiersch TR, Devireddy RV. Subzero water permeability parameters and optimal freezing rates for sperm cells of the southern platyfish, *Xiphophorus maculatus*. Cryobiology. 2005; 50:250–263. [PubMed: 15925577]
23. Rall WF, Czlonkowska M, Barton SC, Polge C. Cryoprotection of day-4 mouse embryos by methanol. J Reprod Fertil. 1984; 70(1):293–300. [PubMed: 6363691]
24. Rall, WF. Advances in the cryopreservation of embryos and prospects for the application to the conservation of salmonid fishes. In: Thorgaard, GH., Cloud, JG., editors. Genetic Conservation of Salmonid Fishes. Plenum Press; New York: 1993. p. 137-158.
25. Ricker JV, Linfor JJ, Delfino WJ, Kysar P, Scholtz EL, Tablin F, Crowe JH, Ball BA, Meyers SA. Equine sperm membrane phase behavior: the effects of lipid-based cryoprotectants. Biol Reprod. 2006; 74:359–365. [PubMed: 16251500]
26. Segovia M, Jenkins JA, Paniagua-Chavez C, Tiersch TR. Flow cytometric evaluation of antibiotic effects on viability and mitochondrial function of refrigerated spermatozoa of Nile tilapia. Theriogenology. 2000; 53:1489–1499. [PubMed: 10898218]
27. Sood R, English MA, Jones M, Mullikin J, Wang DM, Anderson M, Wu D, Chandrasekharappa SC, Yu J, Zhang J, Liu P. Methods for reverse genetic screening in zebrafish by resequencing and TILLING. Methods. 2006; 39(3):220–7. [PubMed: 16828311]
28. Thirumala S, Huang C, Dong Q, Tiersch TR, Devireddy RV. A theoretically estimated optimal cooling rate for the cryopreservation of sperm cells from a live-bearing fish, the green swordtail *Xiphophorus helleri*. Theriogenology. 2005; 63:2395–2415. [PubMed: 15910922]
29. Thirumala S, Campbell WT, Vicknair MR, Tiersch TR, Devireddy RV. Freezing response and optimal cooling rates for cryopreserving sperm cells of striped bass, *Morone saxatilis*. Theriogenology. 2006; 66:964–973. [PubMed: 16574210]

30. Westerfield, M. The Zebrafish Book: A Guide for the Laboratory Use of Zebrafish (*Danio rerio*). University of Oregon Press; Eugene: 2005.

31. Willoughby CE, Mazur P, Peter AT, Critser JK. Osmotic tolerance limits and properties of murine spermatozoa. Biol Reprod. 1996; 55:715–727. [PubMed: 8862792]

32. Wolenski JS, Hart NH. Scanning electron microscope studies of sperm incorporation into the zebrafish (*Brachydanio*) egg. J Exp Zool. 1987; 243:259–273. [PubMed: 3655684]

33. Yang H, Jones C, Varga ZM, Tiersch TR. Development of simplified and standardized protocol for sperm cryopreservation in zebrafish, *Danio rerio,* with potential for high throughput. Theriogenology. 2007; 68(2):128–36. [PubMed: 17544099]

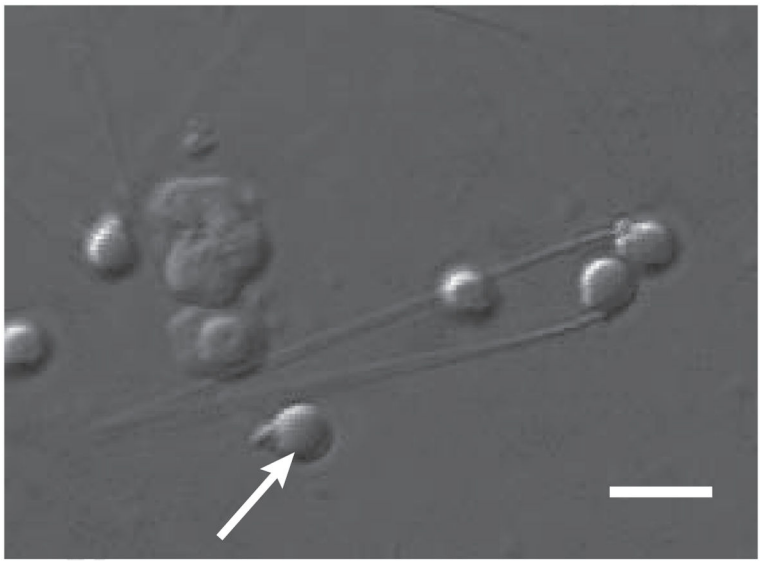

Fig. 1.
Zebrafish sperm morphology. Zebrafish sperm display a prolate head and mid-piece (arrow), and a tail ~30μm in length. Bar = 4 μm.

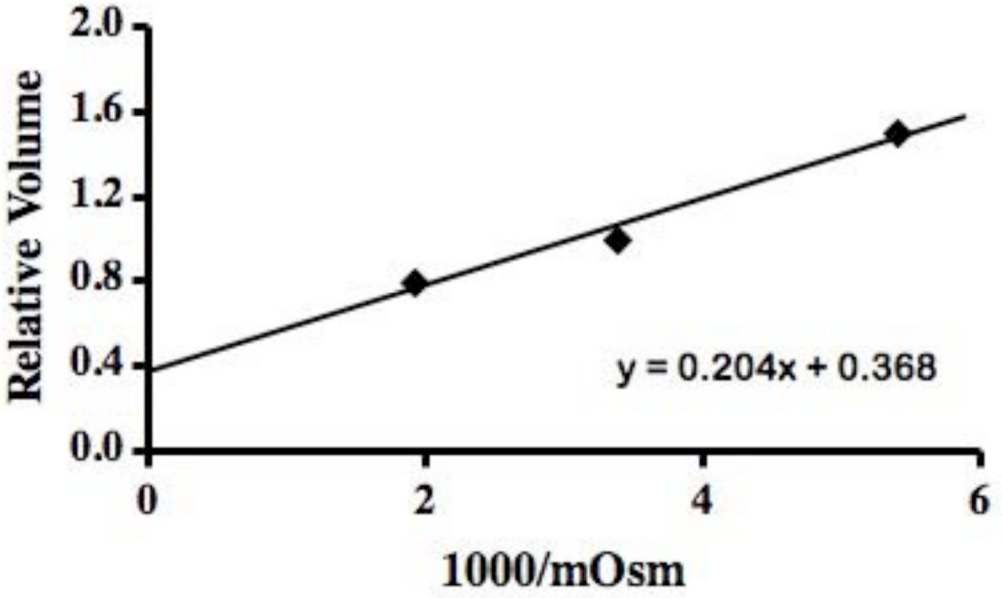

Fig. 2.

Boyle-van't Hoff plot for zebrafish sperm, yielding a value of 0.37 for Vb. This indicates that approximately 37% of the zebrafish sperm cell is not osmotically active.

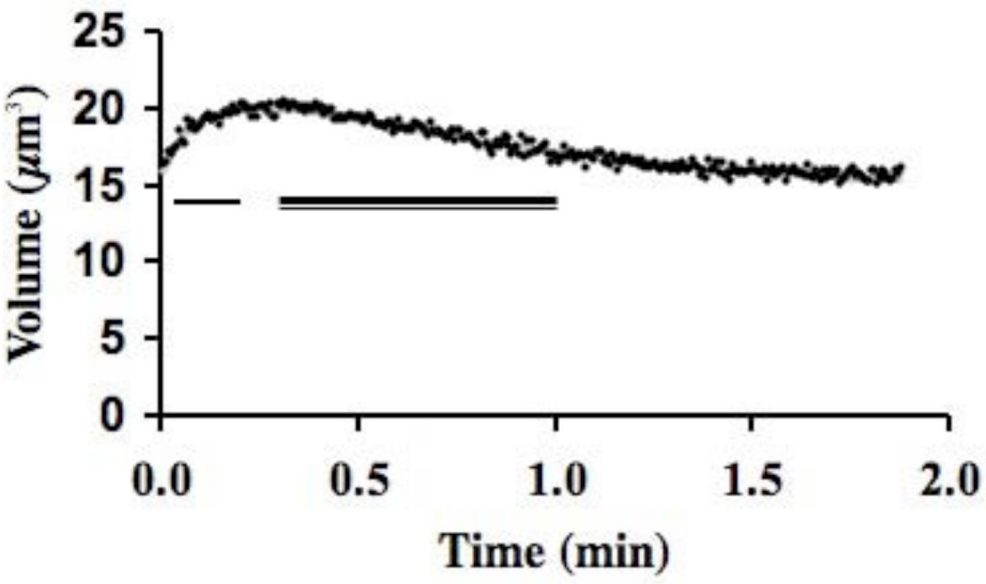

Fig. 3.

Zebrafish sperm, preloaded with 10% dimethyl sulfoxide, were suspended into 300 mOsm/kg HBSS (data, black dots). Water entered the cells (indicated by single line), increasing the volume, and then cryoprotectant and water exited (indicated by double line), decreasing the volume. These data are fit (grey line under the black dots) yielding an Lp of 0.021 ± 0.001 um/min/atm and a Ps of $0.10 \pm 0.01 \times 10^{-3}$ cm/min.

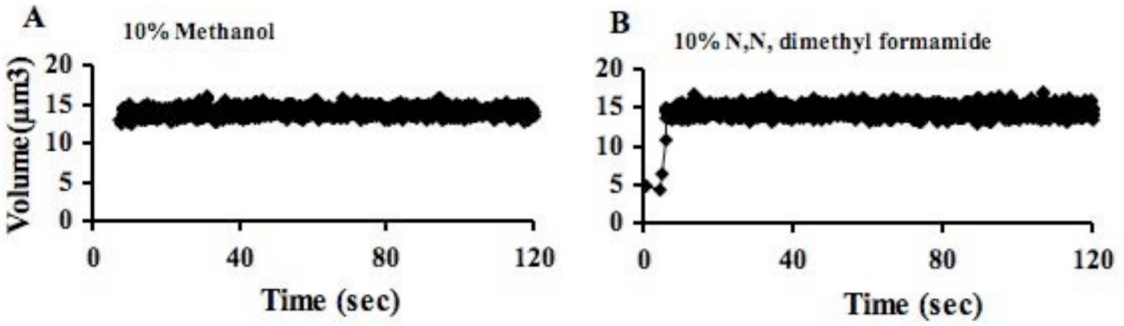

Fig. 4.

Zebrafish sperm, preloaded with (A) 10% methanol and (B) 10% N,N, dimethyl formamide were suspended into 300 mOsm/kg HBSS (data, black dots). No volume change was apparent during either sampling period when the cryoprotectant was exiting the cells.

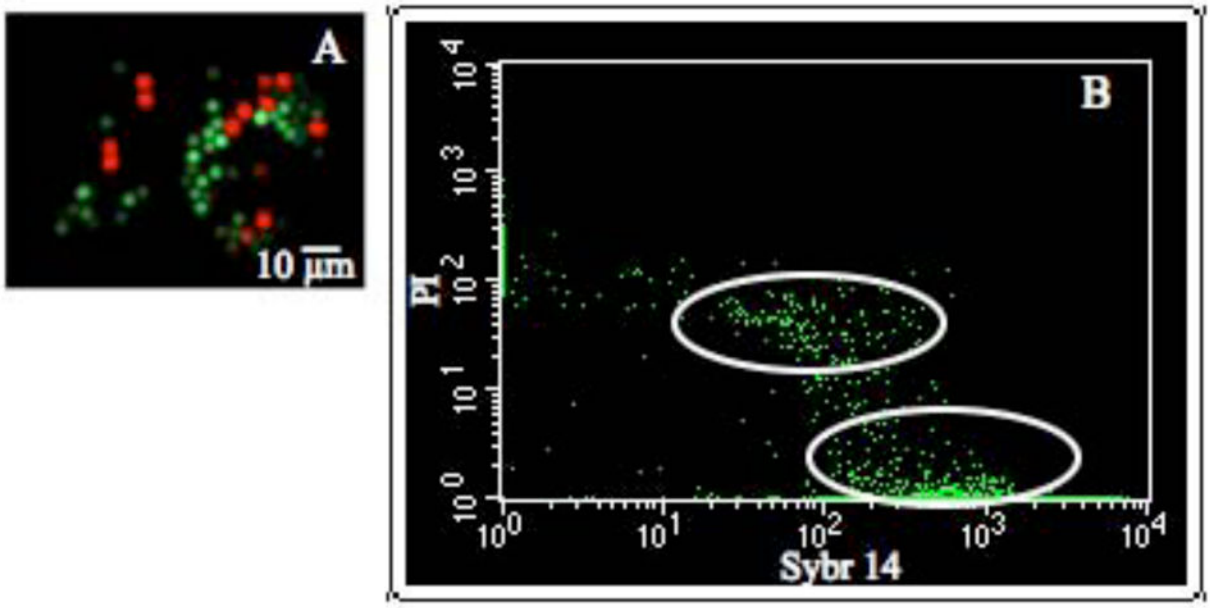

Fig. 5.

The cellular integrity of zebrafish sperm was assessed with fluorescent markers and a flow cytometer. **(A)** Intact cells were identified with SYBR-14 (green) and cells exhibiting membrane damage membrane were identified with propidium iodide (PI, in red), and then imaged using a fluorescence microscope. (**B**) Gated flow cytometry dot plots, showing all the cells in false-colored green. The x-axis displayed SYBR-14, and y-axis PI. Stained zebrafish sperm (shipped 24 h on ice) demonstrated that 92% of the cells were SYBR-14 positive, highlighted by the ellipse in the lower right quadrant, while ~6% of the cells were PI-positive, highlighted by the ellipse in the upper quadrants.

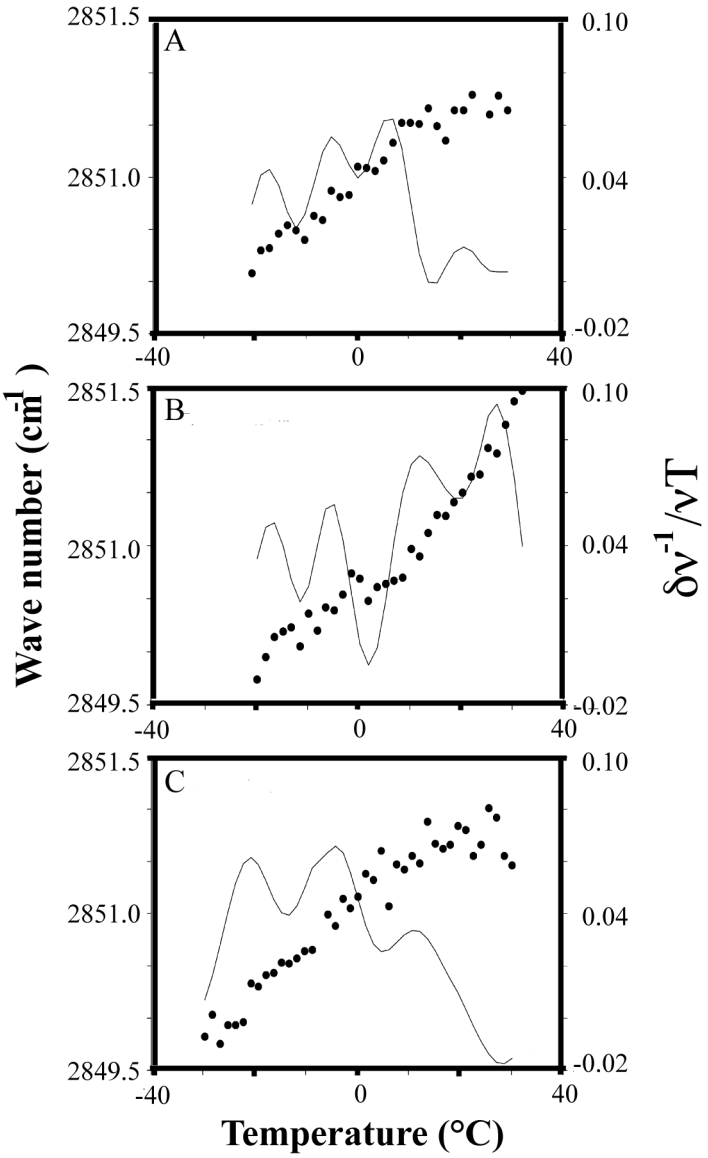

Fig. 6.

Fourier transform infrared spectroscopy (FTIR) of zebrafish sperm. Panel **(A)** shows cooling to ~ −20°C and **(B)** rewarming scans from ~ −20°C of untreated zebrafish sperm, while **(C)** shows a cooling scan of sperm loaded with 10% glycerol in 300 mOsm/kg HBSS. Light lines indicate smoothed first derivatives of the data. Frozen-thawed sperm showed large-scale lipid reorganization and increased cooperativity, or sharpness, of the phase transition peaks relative to fresh sperm. In glycerol, a majority of phase transitions occur at lower temperatures relative to fresh sperm, between −20 and −5 °C. The solution in **(C)** super-cooled to below −30°C and thus did not freeze during this experiment.

Table 1

Zebrafish Sperm Biophysical Parameters

Parameter	Value	Unit
Volume (@300 mOsm)	12.1 ± 0.2	μm^3
Volume/Area Ratio	0.148	µm
Area (from V/A) *	81.8	μm^2
Vb	0.37 ± 0.02	
Lp (in presence of dimethyl sulfoxide, at 21 to 23°C)	0.021 ± 0.001	µm/min/atm
Ps (DMSO)	$0.10 \pm 0.01 \times 10^{-3}$	cm/min
Ps (methanol) **	$\geq 0.3 \times 10^{-3}$	cm/min
Ps (N,N-dimethylformamide) **	$\geq 0.13 \times 10^{-3}$	cm/min

* A = V/(V/A)

** Assuming Lp = 0.021 from dimethyl sulfoxide experiments.

Table 2

Comparative Sperm Parameters

Species	Volume (um^3)	Vb	Reference
Zebrafish	12.1	0.37	This study
Human	25	0.50	[9]
Monkey	28	0.51	[1]
Mouse	56	0.61	[31]